The polycystins are modulated by cellular oxygen-sensing pathways and regulate mitochondrial function

Valeria Padovano[a], Ivana Y. Kuo[b,†], Lindsey K. Stavola[a,†], Hans R. Aerni[a,c], Benjamin J. Flaherty[a], Hannah C. Chapin[a], Ming Ma[d], Stefan Somlo[d], Alessandra Boletta[e], Barbara E. Ehrlich[b], Jesse Rinehart[a,c], and Michael J. Caplan[a,*]

[a]Department of Cellular and Molecular Physiology, [b]Department of Pharmacology, and [d]Department of Internal Medicine, Yale University School of Medicine, New Haven, CT 06520; [c]Systems Biology Institute, Yale University, West Haven, CT 06516; [e]Division of Genetics and Cell Biology, Dibit, San Raffaele Scientific Institute, 20132 Milan, Italy

ABSTRACT **Autosomal dominant polycystic kidney disease is caused by mutations in the genes encoding polycystin-1 (PC1) and polycystin-2 (PC2), which form an ion channel complex that may mediate ciliary sensory processes and regulate endoplasmic reticulum (ER) Ca^{2+} release. Loss of PC1 expression profoundly alters cellular energy metabolism. The mechanisms that control the trafficking of PC1 and PC2, as well as their broader physiological roles, are poorly understood. We found that O_2 levels regulate the subcellular localization and channel activity of the polycystin complex through its interaction with the O_2-sensing prolyl hydroxylase domain containing protein EGLN3 (or PHD3), which hydroxylates PC1. Moreover, cells lacking PC1 expression use less O_2 and show less mitochondrial Ca^{2+} uptake in response to bradykinin-induced ER Ca^{2+} release, indicating that PC1 can modulate mitochondrial function. These data suggest a novel role for the polycystins in sensing and responding to cellular O_2 levels.**

Monitoring Editor
Keith E. Mostov
University of California, San Francisco

Received: Aug 17, 2016
Revised: Nov 10, 2016
Accepted: Nov 15, 2016

INTRODUCTION

Autosomal dominant polycystic kidney disease (ADPKD) affects ~1 in 1000 individuals and is characterized by kidney cyst expansion that destroys surrounding normal tissue (Halvorson *et al.*, 2010). Most cases (85%) result from mutations in Pkd1, which encodes the polycystin-1 protein (PC1), and the remainder result from mutations in Pkd2, which encodes the polycystin-2 protein (PC2; Harris and Torres, 2009). PC1 is a very large, multispanning transmembrane protein (450 kDa) that has been implicated in numerous signaling pathways (Chapin and Caplan, 2010; Harris and Torres, 2014; Ong and Harris, 2015), although its precise function is poorly understood. PC1 undergoes several cleavages, which include an autocatalytic N-terminal cleavage that generates a 150-kDa C-terminal fragment (CTF; Qian *et al.*, 2002). PC2 is a Ca^{2+}-permeable nonselective cation channel and belongs to the transient receptor potential (TRP) channel family (Gonzalez-Perrett *et al.*, 2001). The polycystins (PCs) form a complex that localizes to the plasma membrane (PM), as well as to intracellular compartments, where PC2 can modulate Ca^{2+} release from the endoplasmic reticulum (ER; Koulen *et al.*, 2002). In addition, the PC proteins localize to the primary cilium, where they may participate in mechanosensory or chemosensory pathways (Pazour and Rosenbaum, 2002; Chapin and Caplan, 2010). The interaction between the PCs has been suggested to be important in defining the properties of the ion channel associated with the complex, whether through the modulation of PC2 channel activity or through new emergent channel properties of the complex (Hanaoka *et al.*, 2000; Delmas *et al.*, 2004). The factors that regulate the trafficking, localization, and channel activity of the PCs are unclear. Here we show that PC1 interacts with a component of the cellular O_2-sensing machinery, the prolyl hydroxylase domain–containing protein EGLN3 (or PHD3), and that O_2 levels and the enzymatic activity of the EGLN proteins modulate the subcellular localization and the channel activity of the PC complex.

This article was published online ahead of print in MBoC in Press (http://www.molbiolcell.org/cgi/doi/10.1091/mbc.E16-08-0597) on November 23, 2016.

†These authors contributed equally to this work.

*Address correspondence to: Michael J. Caplan (michael.caplan@yale.edu).

Abbreviations used: ADPKD, autosomal dominant polycystic kidney disease; CTF, C-terminal fragment; OCR, oxygen consumption rate; PC, polycystin.

Moreover, we find that PC1 regulates mitochondrial function, thus suggesting a novel function for the PCs.

RESULTS AND DISCUSSION

The O_2 sensor EGLN3 and O_2 levels affect PC trafficking

To identify genes whose products modulate aspects of PC1 function, including its trafficking and the cleavage and nuclear translocation of its C-terminal tail (CTT; Chapin and Caplan, 2010), we designed a cell-based, high-content, genome-wide, small interfering RNA (siRNA)–based screen that employed HEK293 cells expressing tagged versions of PC1 and PC2. High-throughput confocal microscopy was used to quantify the fraction of PC1 present at the PM. EGLN3 was identified as a protein that profoundly influences PC1 trafficking to the cell surface. EGLN3 knockdown significantly increased the fraction of PC1 that localized to the PM (see the Supplemental Experimental Procedures for details concerning the design of the screen and the criteria for hit selection). The three paralogues of the EGLN proteins serve as cellular O_2 sensors, which regulate the hypoxia response pathway. In the presence of O_2, EGLN proteins hydroxylate proline residues on the hypoxia-induced factor HIF1α. This modification targets HIF1α for degradation (Jaakkola *et al.*, 2001). Although it shares overlapping functions with the other two paralogues (EGLN1 and EGLN2), EGLN3 has the widest range of non-HIF targets (Jaakkola and Rantanen, 2013).

Because the screen was performed in nonpolarized HEK293 cells, we assessed whether EGLN3 knockdown influenced PC1 trafficking in polarized, ciliated LLC-PK_1 cells overexpressing both PC1 and PC2. An extracellular Flag epitope appended to the N-terminus of our PC1 construct allowed us to perform surface immunofluorescence (IF) labeling of only the pool of PC1 that is localized to the apical and ciliary membranes (Chapin *et al.*, 2009). EGLN3 knockdown (Supplemental Figure S1A) increased the amount of PC1 at the apical surface (Figure 1A). Moreover, we found that the 150-kDa CTF that is generated by the autocatalytic N-terminal cleavage of PC1 (Qian *et al.*, 2002) interacts with EGLN3 both in transfected cells and in mouse renal tissue in vivo (Figure 1B and Supplemental Figure S1B). Coimmunoprecipitation (coIP) experiments showed that PC1 also interacts to a lesser extent with EGLN1 and EGLN2 (Supplemental Figure S1C). To avoid any confounding effects from the potential compensatory activities of the EGLN1 and 2 proteins, we used pharmacological approaches that inhibit all three of the EGLN isoforms rather than an isoform-specific knockdown approach to examine the consequences for PC1 distribution and function of reduced EGLN activity.

To test whether the PC1-EGLN3 interaction was dependent on EGLN3 activity, we inhibited EGLN3 function by 1) incubating cells in hypoxic conditions (5% CO_2 and 95% N_2) for 2 h; 2) by incubating them for 24 h in the presence of the hypoxia-mimicking compound $CoCl_2$ to simulate prolonged hypoxia; or 3) by incubating them for 24 h with the pan EGLN inhibitor dimethyloxalylglycine (DMOG). We also incubated cells in hyperoxic conditions to increase O_2 availability and hence enhance EGLN3 activity. We found that the PC1-EGLN3 interaction is not dependent on EGLN3 activity because EGLN3 coimmunoprecipitates with the PC1 CTF regardless of the treatment (Figure 1B). Moreover, we found that PC2 also coimmunoprecipitates with EGLN3 (Supplemental Figure S2A). Because PC1 and PC2 interact with one another, these data do not reveal which of these proteins interacts with EGLN3. To determine whether EGLN3 can assemble with the cytoplasmic domains of PC1, we generated two constructs that embody distinct portions of the cytosolic regions of PC1. One of these is a concatenation of the five cytosolic loops of PC1 (PC1 C.L.1-5), in which each loop is connected to its neighbors by a flexible linker. The other corresponds to the PC1 CTT. Of interest, EGLN3 interacts with both PC1 C.L.1-5 and CTT (Supplemental Figure S2B) when it is coexpressed with either of these PC1 cytoplasmic domain constructs in HEK cells. These data suggest that EGLN3 participates in associations with multiple portions of the PC1 cytoplasmic domain. Although these data do not rule out the possibility that EGLN3 can also associate with PC2, they demonstrate that the cytoplasmic sequences of PC1 are sufficient to participate in interactions with EGLN3.

The effect of EGLN3 knockdown on PC1 localization suggested that O_2 levels might affect PC1 trafficking. To test this hypothesis, we incubated LLC-PK_1 cells overexpressing PC1 and PC2 in a hypoxia chamber for 2 h or in the presence of the hypoxia-mimicking compound $CoCl_2$ for 24 h and found that both treatments induced an increase in the amount of PC1 localized to the apical surface and to the primary cilium (Figure 1C). Pretreatment with brefeldin A (BFA) for 30 min prevented the increase in the size of the PC1 surface pool (Figure 1D), indicating that the increase in surface staining is likely due to an increase in the trafficking of newly synthesized PC1 from the ER rather than to a reduced rate of endocytosis or degradation of the apical pool of PC1. The PCs traffic together in a complex (Chapin *et al.*, 2010; Kim *et al.*, 2014), and so we assessed whether hypoxia had the same effect on PC2 trafficking. We performed surface biotinylation after 2 h of hypoxia or 24 h of $CoCl_2$ treatment and found that PC2 localization to the cell surface increased significantly after 2 h of hypoxia (80% increase in surface PC2) but not after the 24-h $CoCl_2$ treatment, suggesting that the effect of hypoxia on PC2 localization may be rapid and transient (Figure 1E). Quantification of ciliary PC2, performed by IF microscopy as described for PC1 (see Supplemental Figure S4), showed that hypoxic conditions did not increase the quantity of PC2 in the primary cilium (as shown in the graph in Figure 1E).

PC1 is modified by EGLN

To test whether PC1 is an EGLN substrate, we immunoprecipitated hemagglutinin (HA)-tagged PC1 from HEK cells overexpressing PC1 and PC2. Proline hydroxylation was assessed by Western blotting with an anti–hydroxylated proline (OH-Pro) antibody that has been used to assess the proline hydroxylation states of HIF and of several other proteins (Jung *et al.*, 2012; Luo *et al.*, 2014). We found that hydroxylated proline residues are present in the PC1 CTF (Figure 2A). No consistent hydroxylation signal was detected on PC2. The extent of PC1 proline hydroxylation is reduced after 48 h of treatment with DMOG (Figure 2A, graph). PC1 hydroxylation also occurs in renal tissue in vivo. We used a Pkd1-BAC model (Figure 2B, top) expressing three copies of Pkd1 (Fedeles *et al.*, 2011) and a knock-in mouse model expressing physiological levels of Pkd1 (Figure 2B, bottom; Wodarczyk *et al.*, 2009). In both cases, the PC1 protein is HA tagged at its C-terminus. The PC1 protein immunoprecipitated from both animal models was detected in Western blots probed with the antibody directed against OH-Pro. The presence of OH-Pro was also verified by mass spectrometry (MS) performed on the PC1 CTF immunoprecipitated from HEK293 cells overexpressing PC1 and PC2, which revealed that at least five peptides in the cytosolic regions of PC1 were hydroxylated at one or more residues (mapped onto a schematic representation of the PC1 CTF in Figure 2C; details in Supplemental Table S1). A representative tandem MS for one of the identified peptides, GELYRPAWEPQDYEMVELFLR, is shown in Figure 2D. This spectrum depicts the *y* and *b* ions that result from the progressive fragmentation of the specified peptide. The mass-to-charge (*m*/*z*) ratio of associated fragment ions is consistent with the presence of two OH-Pro residues in the positions indicated. The

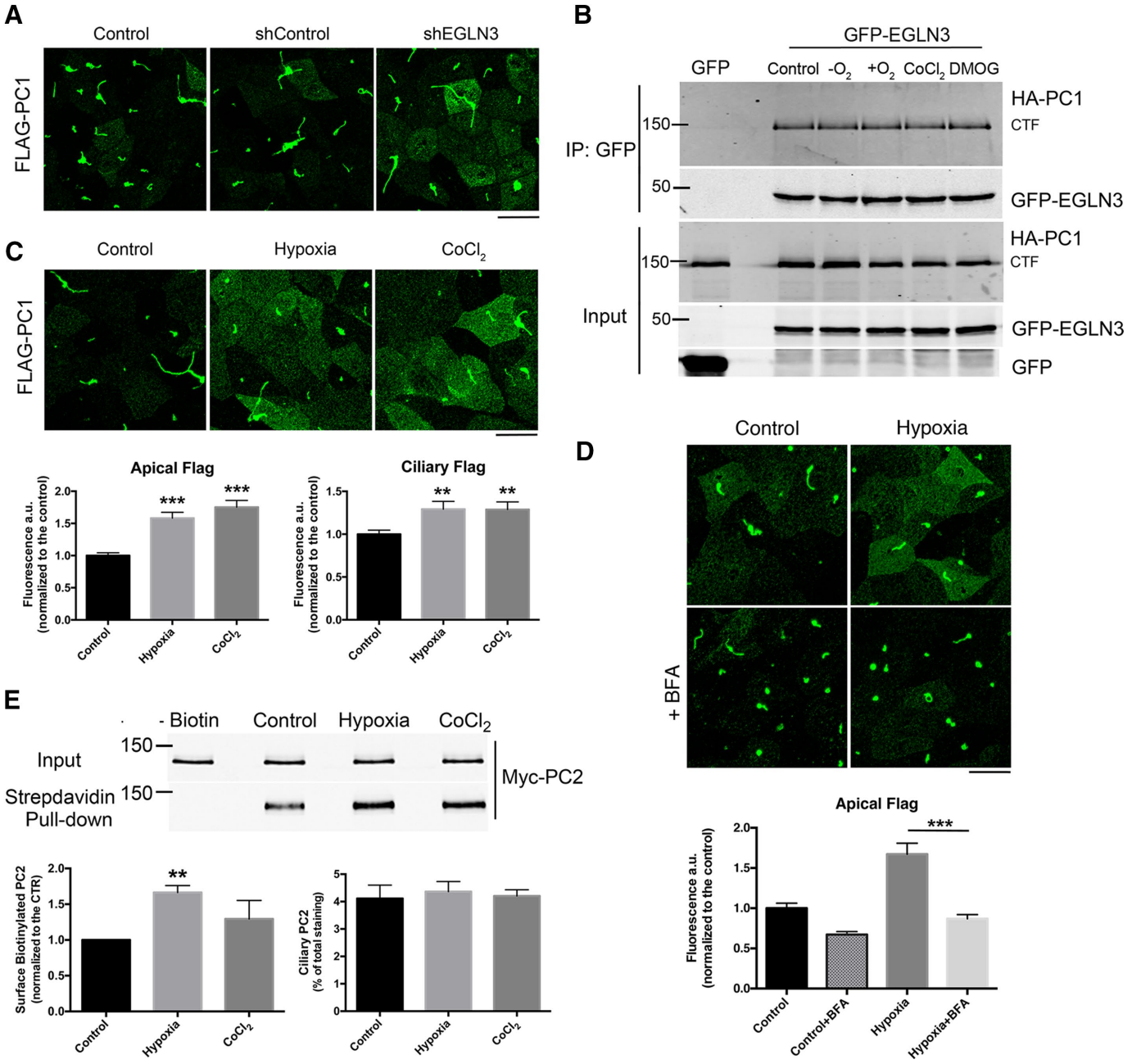

FIGURE 1: EGLN3 expression and O_2 levels affect PC trafficking. (A) Surface IF analysis of N-terminally Flag-tagged PC1 using an anti-Flag antibody in LLC-PK_1 cells overexpressing PC1 and PC2, which were knocked down or not for EGLN3 expression. (B) CoIP of GFP-EGLN3 and PC1 in HEK293 cells; cells were incubated in hypoxia ($-O_2$) or hyperoxia ($+O_2$) for 2 h or with 1 mM DMOG or 200 μM $CoCl_2$ for 24 h. (C) Surface IF of PC1 expressed in LLC-PK_1 cells incubated under control conditions, in hypoxia for 2 h, or with $CoCl_2$ for 24 h; the graphs show the quantification of three independent experiments. (D) Surface IF of PC1 expressed in LLC-PK_1 cells incubated under control conditions or in hypoxia for 2 h with or without 20 μM BFA. (E) Surface biotinylation of PC2 in LLC-PK_1 cells overexpressing PC1 and PC2 that were incubated under control conditions, in hypoxia for 2 h, or with $CoCl_2$ for 24 h; left graph, quantification of four independent surface biotinylation experiments; right graph, quantification of ciliary PC2 detected by IF ($n = 4$). For A, C, and D, a maximum intensity projection of a *z*-stack taken with a 0.69-μm step is shown. Bars, 20 μm. Data are shown as mean ± SEM. $^{**}p < 0.01$ and $^{***}p < 0.001$ determined by *t* test.

large size and consequent complex fragmentation pattern of PC1 made it difficult to determine whether hydroxylation of individual peptides varied as a consequence of DMOG or hypoxia treatment. Taken together with the results obtained with the OH-Pro antibody, however, these data strongly support the conclusion that PC1 is proline hydroxylated under physiological circumstances.

O_2 levels regulate the channel activity of the PC complex

A number of proteins have been found to be EGLN substrates (Xie *et al.*, 2009), including the TRP channel TRPA1 (Takahashi *et al.*, 2011). EGLNs inhibit TRPA1 channel activity in normoxic conditions through hydroxylation of a specific proline residue, whereas reduced O_2 levels lead to activation of the channel. The O_2 levels also

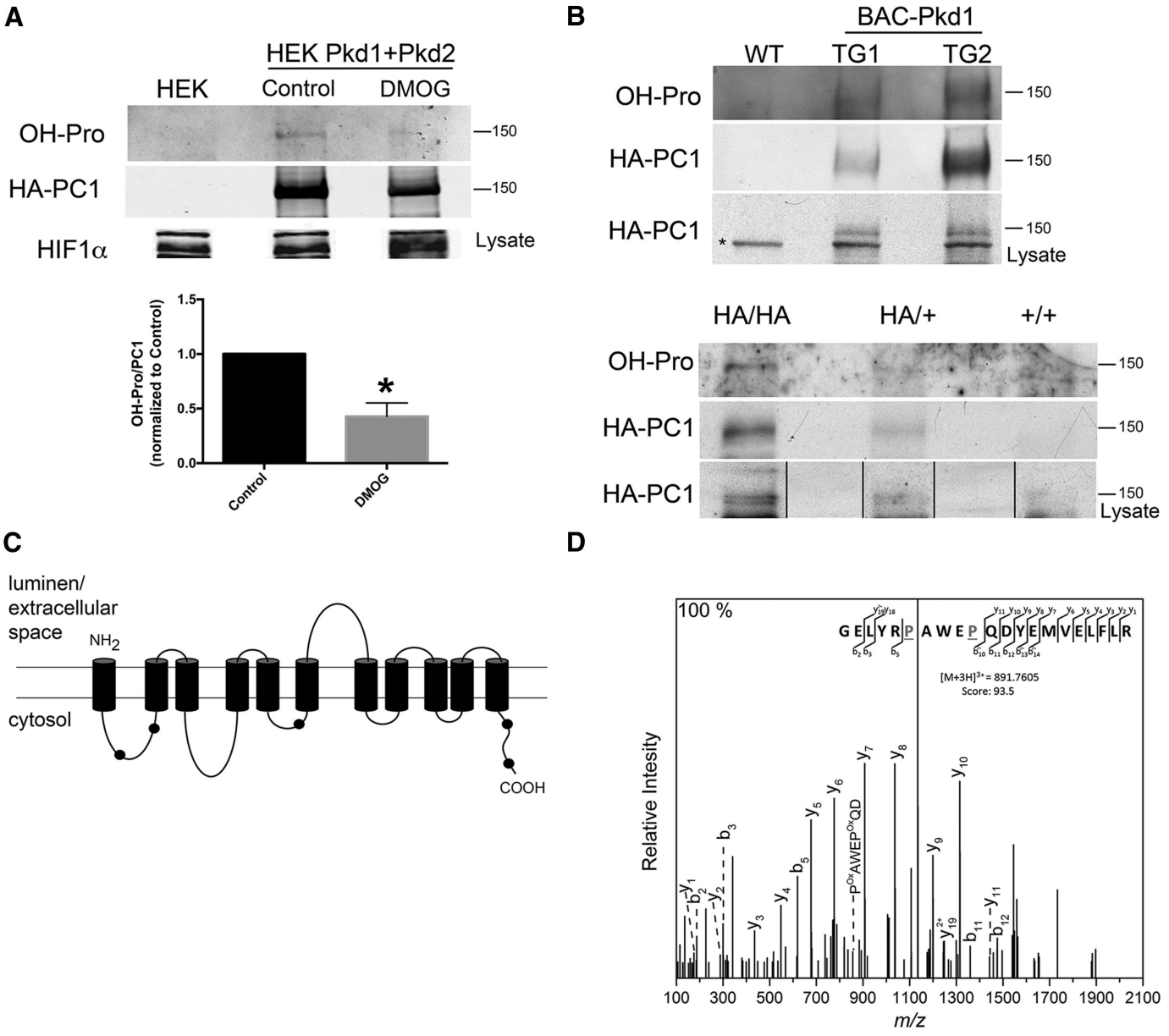

FIGURE 2: PC1 proline hydroxylation. (A) Western blot analysis to detect the presence of OH-Pro on PC1 that was immunoprecipitated from HEK293 cells that overexpress PC1 and PC2 and were untreated (Control) or treated with 1 mM DMOG for 48 h; the graph shows the quantification of three independent experiments; *$p < 0.05$. (B) Western blot analysis of OH-Pro on PC1 that was immunoprecipitated from kidneys of mice expressing 3xHA-tagged Pkd1 (top; kidneys from two different transgenic animals, TG1 and TG2, and one wild-type mouse [WT]). The asterisk indicates a nonspecific band recognized by the anti-HA antibody in mouse tissue. Western blot analysis of OH-Pro on PC1 immunoprecipitated from kidneys of heterozygous (HA/+) and homozygous (HA/HA) HA-tagged PC1 knock-in mice; material from a wild type mouse is also shown (bottom). (C) Schematic representation of the PC1 CTF, showing the localization of the peptides containing OH-Pro that were identified by MS (black dots). The position and sequence of the peptides corresponding to each black dot are presented in Supplementary Table S1. (D) Tandem MS of the peptide GELYRPAWEPQDYEMVELFLR from PC1 confirming the presence of two OH-Pro residues (P). Characteristic *b* and *y* ions and internal ions were annotated for clarity.

modulate the cell surface expression of TRPA1 (Takahashi *et al.*, 2011). PC2 is a Ca^{2+}-permeable cation TRP channel (Gonzalez-Perrett *et al.*, 2001) that can mediate or modulate Ca^{2+} release from intracellular stores (Koulen *et al.*, 2002). In addition, several membrane spans of PC1 share structural homology with the TRP family. Interaction between PC1 and PC2 may be important in modulating the localization or the intrinsic channel properties of PC2 (Hanaoka *et al.*, 2000; Delmas *et al.*, 2004; Casuscelli *et al.*, 2009). To test whether EGLN catalytic activity affects PC2 channel activity, we performed single-channel recordings using bilayer membranes into which were fused ER microsomes prepared from untransfected LLC-PK_1 cells or from LLC-PK_1 cells overexpressing PC1 and PC2. These cells had been treated under control conditions, exposed to a low-O_2 environment for 2 h, or treated with DMOG overnight. The presence of both PCs in the microsome fraction was confirmed by Western blot analysis (Supplemental Figure S3A). Microsomes isolated

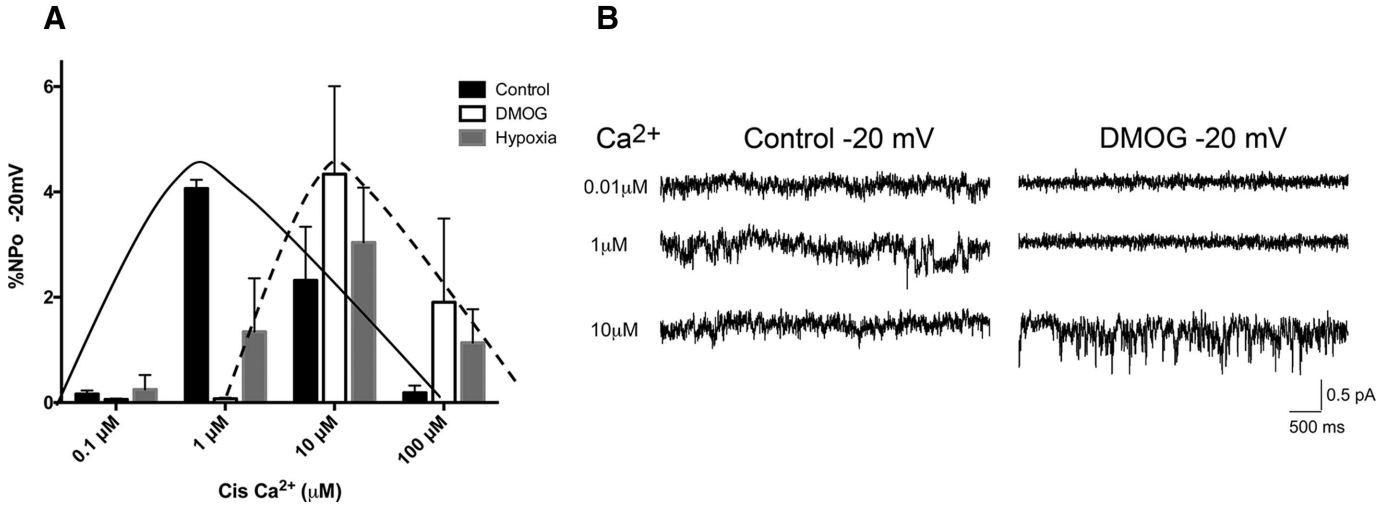

FIGURE 3: EGLN activity regulates PC channel activity. (A) Single-channel recording performed on microsomes isolated from LLC-PK$_1$ cells overexpressing PC1 and PC2 and incubated under control conditions, in hypoxia for 2 h, or with 1 mM DMOG 24 h; the solid line highlights the Ca^{2+} sensitivity pattern of channel activity in control conditions, and the dashed line outlines the shift in Ca^{2+} sensitivity induced by DMOG and hypoxia treatments. The O_2 effect on channel activity is statistically significant; $p = 0.0018$ as assessed by two-way analysis of variance. (B) Representative traces of Ca^{2+} currents recorded using microsomes isolated from cells overexpressing PC1 and PC2 that were untreated or treated for 24 h with 1 mM DMOG. Data are representative of three different microsome preparations.

from untransfected cells did not show channel activity under the conditions used. Of interest, inhibition of EGLNs by hypoxia or DMOG treatment altered the PC channel properties, inducing a rightward shift in the sensitivity of the channel to activation by Ca^{2+} (Figure 3). Thus PC channel activity at resting cytosolic Ca^{2+} concentrations would be expected to be substantially reduced in a low-O_2 environment. The decreased Ca^{2+} sensitivity of the PC channel, together with the redistribution of the PCs from the ER to the cell surface, may result in a reduction in the magnitude of PC-associated ER Ca^{2+} release under hypoxic conditions.

PC1 regulates mitochondrial function

Recent data document substantial metabolic perturbations in ADPKD-affected cells and tissues (Rowe *et al.*, 2013; Menezes *et al.*, 2016). Some of these alterations are associated with high levels of aerobic glycolysis, reminiscent of the Warburg effect in tumor cells (Vander Heiden *et al.*, 2009). The mechanisms responsible for this behavior have not been elucidated. Ca^{2+} release from the ER and its uptake by mitochondria regulates oxidative phosphorylation (OXPHOS) by activating critical enzymes, including pyruvate dehydrogenase (PDH), α-oxoglutarate dehydrogenase, and isocitrate dehydrogenase (McCormack and Denton, 1979; Cardenas *et al.*, 2010; Rizzuto *et al.*, 2012). Our data demonstrate that the PC channel activity is reduced during hypoxia. These observations together suggest the interesting possibility that the PCs may play a role in regulating mitochondrial OXPHOS. To test this hypothesis, we measured O_2 consumption rate (OCR) in Pkd1$^{-/-}$ and Pkd1$^{flox/-}$ mouse renal proximal tubule cell lines, which completely lack or are heterozygous for PC1 expression, respectively (Merrick *et al.*, 2012). We found that Pkd1$^{-/-}$ cells manifest reduced OCR compared with Pkd1$^{flox/-}$ cells (Figure 4A), consistent with a reduction in the quantity of OXPHOS performed by these cells. To determine whether EGLN-mediated effects on PC1 are implicated in OXPHOS regulation, we measured OCR in Pkd1$^{-/-}$ and Pkd1$^{flox/-}$ cells treated with DMOG. We found that EGLN inhibition affected mitochondrial activity and induced a significant reduction in both the basal and maximal OXPHOS performed by PC1-expressing cells (Figure 4B). Cells lacking PC1 expression showed a nonsignificant decrease after DMOG treatment only in their maximal respiration, and no effect on basal respiration was observed in these cells. These data indicate that PC1 expression and EGLN activity play a physiologically important role in the regulation of baseline respiration. Moreover, treatment with dichloroacetate (DCA), an inhibitor of pyruvate dehydrogenase kinase, and therefore an OXPHOS activator (Cardenas *et al.*, 2010), induced a moderate but significant increase in the OCR in cells lacking PC1 (Figure 4C). DCA had no effect on OCR in PC1-expressing cells, suggesting that pharmacological stimulation of mitochondrial respiration can partially rescue the metabolic perturbations observed in the absence of PC1.

Because PCs modulate ER Ca^{2+} release and mitochondrial Ca^{2+} uptake regulates OXPHOS, we tested whether mitochondrial uptake is perturbed in cells lacking PC1 expression. We performed confocal live imaging on Pkd1$^{-/-}$ and Pkd1$^{flox/-}$ cells transfected with the MTS-RCaMP, a mitochondria-targeted version of the genetically encoded Ca^{2+} sensor RCaMP1h (Akerboom *et al.*, 2013; Supplemental Figure S3B). Stimulation of ER Ca^{2+} release by treatment with bradykinin (performed in the absence of extracellular Ca^{2+}) induced significantly higher mitochondrial Ca^{2+} uptake in cells expressing PC1 (Figure 4, D and E). This difference was not due to a difference in the size of ER Ca^{2+} stores because treatment with ionomycin, which has been shown to release Ca^{2+} from ER stores (Morgan and Jacob, 1994), induced the same mitochondrial Ca^{2+} uptake in both cell lines in the absence of extracellular Ca^{2+} (unpublished data). Moreover, cytosolic calcium measurements using the cell-permeant dye Fluo4-am (performed in the presence of extracellular Ca^{2+}) showed the same response to bradykinin in both cell lines (Supplemental Figure 3C), thus excluding the possibility that PC1 expression affects the magnitude of cell-surface bradykinin receptor expression or function. Further supporting the hypothesis that the PCs participate in the regulation of mitochondrial Ca^{2+} levels, we found that both PC1 and PC2 cofractionate with mitochondria-associated ER membranes (MAMs; Figure 4F), regions of close

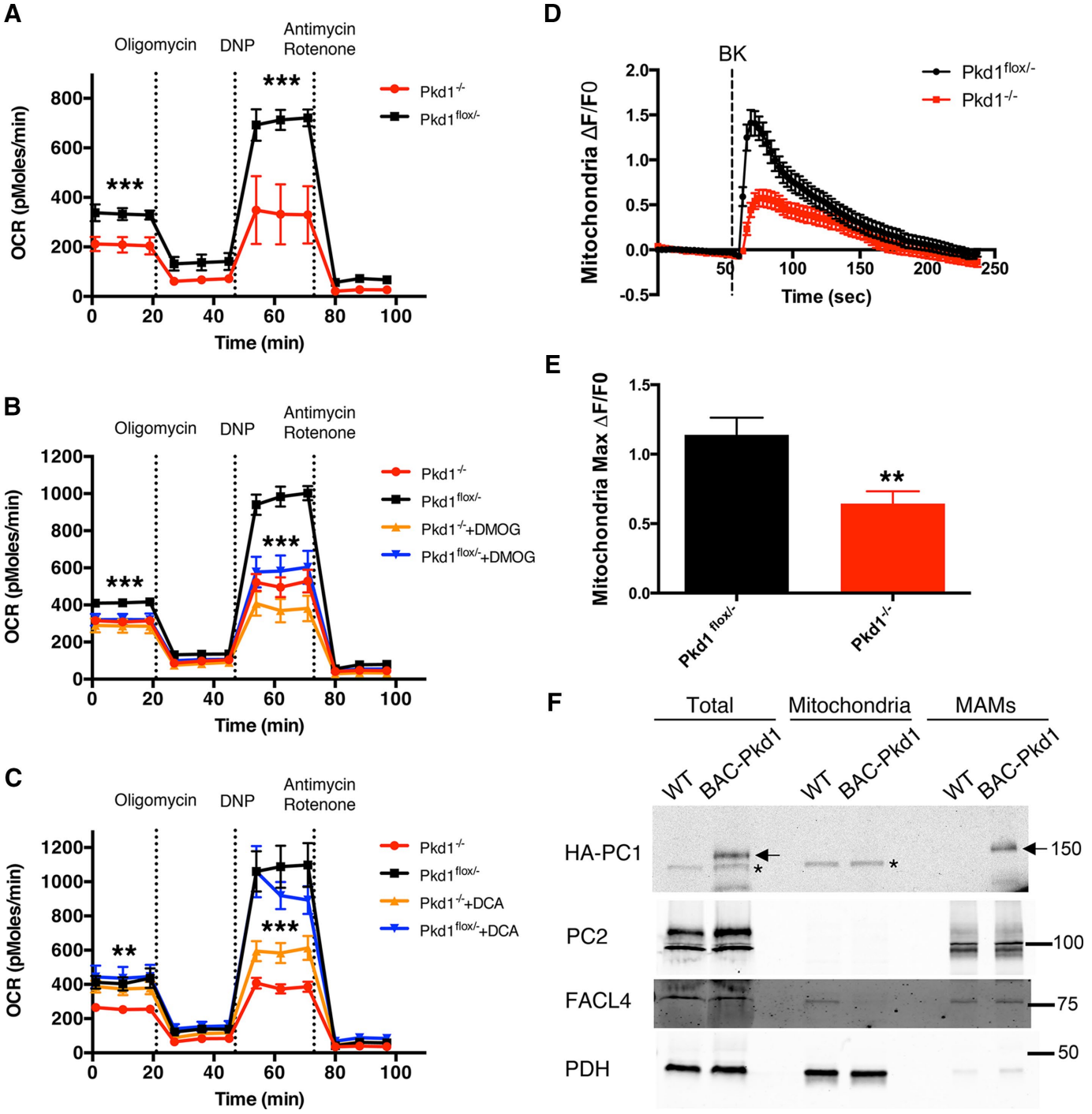

FIGURE 4: PC1 expression affects mitochondrial function and Ca^{2+} uptake. (A) OCR (picomoles/minute) in $Pkd1^{-/-}$ and $Pkd1^{flox/-}$ proximal tubule cells. (B) OCR in $Pkd1^{-/-}$ and $Pkd1^{flox/-}$ cells treated under control conditions or with 1 mM DMOG overnight. DMOG reduces OCR in $Pkd1^{flox/-}$ cells but not in $Pkd1^{-/-}$ cells. (C) OCR in $Pkd1^{-/-}$ and $Pkd1^{flox/-}$ cells under control conditions or after 5 mM DCA treatment for 1 h. DCA increases OCR in $Pkd1^{-/-}$ cells but not in $Pkd1^{flox/-}$ cells. OCR values from three independent experiments were normalized to total DNA content to account for variations in cell number. (D) Representative $\Delta F/F_0$ graph showing bradykinin (BK)-induced mitochondrial Ca^{2+} uptake in $Pkd1^{-/-}$ and $Pkd1^{flox/-}$ cells in the absence of extracellular Ca^{2+} (18 cells from one experiment). (E) The maximum $\Delta F/F_0$ fluorescence induced by BK (three experiments; 37 $Pkd1^{flox/-}$ and 57 $Pkd1^{-/-}$ cells analyzed). (F) Western blot analysis of total (60 µg of proteins), mitochondrial (12 µg), and MAM (12 µg) fractions blotted with antibodies directed against HA (to reveal PC1), PC2, the mitochondrial marker PDH, and the MAM marker FACL4. The asterisk indicates a nonspecific band generated by the anti-HA antibody in mouse tissue; the arrows represent the specific HA-PC1 band. Data are shown as mean ± SEM. *$p < 0.05$, **$p < 0.01$, and ***$p < 0.001$ determined by t test.

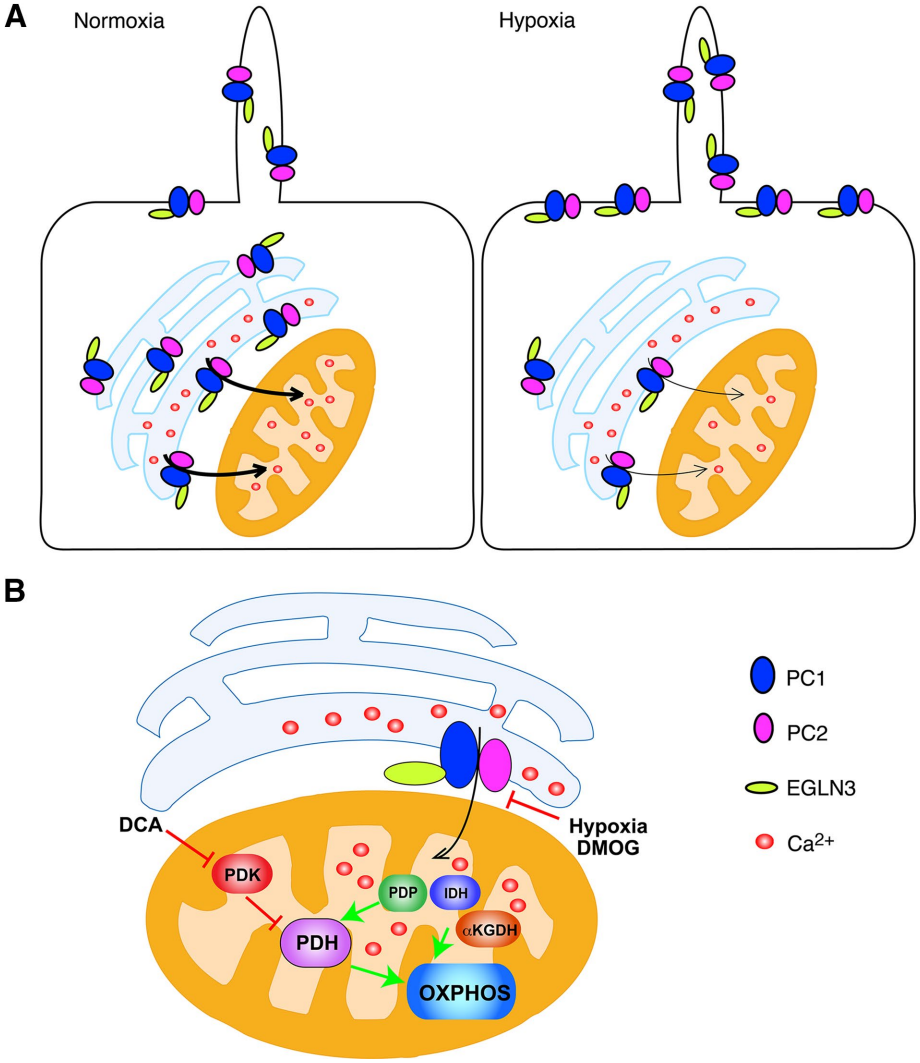

FIGURE 5: Models of the EGLN3-dependent regulation of PC trafficking and the influence of EGLN3 and the PCs on the regulation of OXPHOS. (A) Regulation of PC trafficking and channel activity. In the presence of O_2, the fraction of the PC complex localized to the ER may facilitate ER Ca^{2+} leak and its uptake by the mitochondrion. Under hypoxic conditions, the PC complex translocates to the PM, and its Ca^{2+} sensitivity is reduced, possibly resulting in a reduction in ER Ca^{2+} leak. (B) Regulation of OXPHOS by the PC complex. ER-to-mitochondrion Ca^{2+} leak, facilitated by the PC complex, may activate PDH, IDH, or αKGDH and thus OXPHOS. Decreased O_2-dependent prolyl hydroxylation of the PC complex, as a result of hypoxia or DMOG-mediated inhibition of EGLN activity, may decrease ER-to-mitochondrion Ca^{2+} leak, resulting in decreased OXPHOS. Activation of PDH, through pharmacological treatment with the PDH kinase inhibitor DCA at least partially bypasses the need for PC function and restores OXPHOS activity. αKGDH, α-ketoglutarate dehydrogenase; IDH, isocitrate dehydrogenase; PDH, pyruvate dehydrogenase; PDK, PDH kinase; PDP, PDH phosphatase.

apposition between the ER and the mitochondrial membrane that represent hot spots for the regulation of Ca^{2+} transfer between these organelles (Patergnani *et al.*, 2011). These results indicate that the PC complex can affect mitochondrial Ca^{2+} uptake and function.

Our findings reveal a novel mechanism that regulates the trafficking and channel activities of PCs and places the complex in the cellular O_2-sensing pathway. The O_2 levels affect the localization of the PC proteins and the Ca^{2+} sensitivity of their associated channel activity, suggesting that under normoxic conditions, the PC channel complex is triggered at relatively lower Ca^{2+} concentrations, permitting it to participate in ER Ca^{2+} release under normal levels of cytosolic Ca^{2+} (Figure 5A). This PC complex–mediated Ca^{2+} release can, in turn, affect mitochondrial Ca^{2+} uptake and therefore stimulate oxidative metabolism (Figure 5B). Conversely, under hypoxic conditions, the PC channel translocates to the cell surface and is less sensitive to activation by Ca^{2+}, which results in less PC-mediated ER Ca^{2+} release in the presence of normal cytosolic Ca^{2+} concentrations and thus less Ca^{2+}-dependent OXPHOS. According to this model, lack of PC1 expression may mimic a low-O_2 environment, leading to altered mitochondrial function, which results in a lower OCR. Consistent with this possibility, pharmacological activation of pyruvate dehydrogenase by treatment with DCA partially reverses the reduced OCR that is observed in cells lacking PC1 expression. Therefore, our results provide a possible explanation for at least some aspects of the previously observed metabolic perturbations in ADPKD-affected cells and tissues (Rowe *et al.*, 2013).

MATERIALS AND METHODS

Hypoxia/hyperoxia and brefeldin A treatment

The hypoxic/hyperoxic environment was created using a hypoxia chamber (Billups-Rothenberg, San Diego, CA) by flowing different gas mixtures. For the hypoxia experiments, we used a 95% N_2, 5% CO_2 mixture, and for hyperoxia, we used an 85% O_2, 5% CO_2, and 10% N_2 mixture. We ran the gas for 15 min at 2 psi and then clamped both the inlet and the outlet ports simultaneously to seal the chamber. The chamber containing the cells was incubated for 2 h at 37°C. The BFA-treated samples were preincubated in the presence of 20 μM BFA for 30 min before the hypoxia and during the 2-h incubation in the hypoxia chamber.

Microsome preparation and single-channel recordings

LLC-PK1 cells overexpressing PC1 and PC2 were grown to confluence in 100-mm dishes (Corning), treated as indicated, collected by scraping into phosphate-buffered saline, and centrifuged at 200 × *g* for 5 min. Cell pellets were resuspended in 1 ml of microsome buffer (250 mM sucrose, 10 mM Tris, pH 7.6, 50 mM NaCl) plus protease inhibitor cocktail (Roche), probe sonicated three times for 10 s each (40% power, 4°C), and centrifuged for 10 min at 8000 × *g* at 4°C. Supernatants were ultracentrifuged at 100,000 × *g* for 45 min at 4°C. Pellets containing PC1- and PC2-enriched ER microsomes were resuspended in 100 μl of microsome buffer.

Microsomes from cells subjected to differing O_2 environments or DMOG treatment (1 mM for 24 h) were fused to lipid bilayers as described (Koulen *et al.*, 2002). Experiments were performed with 250 mM 4-(2-hydroxyethyl)-1-piperazineethanesulfonic acid (HEPES)–Tris solution, pH 7.35, on the *cis* side and 250 mM HEPES,

55 mM $Ba(OH)_2$ solution, pH 7.35, on the *trans* side. Incorporation of channels was monitored by the addition of KCl on the *cis* side. Once incorporation of channels was established, the solution on the *cis* side was exchanged with 10× volume of 250 mM HEPES-Tris solution, pH 7.35. PC2 channels were then activated by the sequential addition of Ca^{2+} to the *cis* side. Channel activity was recorded for 2 min at each Ca^{2+} concentration under voltage-clamp conditions (–20 mV holding potential) using a Bilayer Clamp BC-525C (Warner Instruments, Hartford, CT), filtered at 1 kHz, and digitized at 5 kHz. Data were acquired and analyzed with pClamp9 (Axon Instruments, Burlingame, CA). Channel characteristics (open probability, Ca^{2+} sensitivity, current amplitude) were compared with previously obtained traces of PC2.

Oxygen consumption

The OCR was measured using an XF24 extracellular analyzer (Seahorse Bioscience, North Billerica, MA). Cells were seeded at confluent density in XF24 cell culture microplates (Seahorse Bioscience) the day before the experiment. During the assay, cells were sequentially exposed to oligomycin (10 μg/ml), 2,4-dinitrophenol (1 mM), and antimycin A (10 μM) plus rotenone (10 μM). After each injection, OCR was measured for 3 min, and the medium was mixed for 2 min and again measured for 3 min. Every point in each experiment represents an average of nine (three experiments in triplicate) different wells. Data were normalized for DNA content to account for variations in cell number by performing Hoechst 33342 (Molecular Probes) staining, followed by fluorescence reading in an Infinite M1000 PRO microplate reader (Tecan, San Jose, CA).

Genome-wide siRNA screen

The Genome Wide siRNA screen was performed in collaboration with the Yale Center for High Throughput Cell Biology.

Additional details on the experimental procedures are given in the Supplemental Experimental Procedures.

ACKNOWLEDGMENTS

We thank Deborah Smith, Adrian Poffenberger, Marie-Aude Guie, and Michael Wyler for invaluable contributions to the design and execution of the siRNA screen, Michael Jurczak and Gerald Shulman for generously making available their expertise and equipment for the OCR measurements, and Anita Aperia and members of her laboratory for designing and generously providing the MTS-RCaMP construct. Finally, we thank the members of the Caplan laboratory for helpful suggestions and in particular Vanathy Rajendran for help with the execution of experiments. This work was supported by the Polycystic Kidney Disease Research Center at Yale University (National Institutes of Health Grant P30 DK090744) and by Department of Defense Peer Reviewed Medical Research Program Grant W81XWH-10-1-0504.

REFERENCES

Akerboom J, Carreras Calderon N, Tian L, Wabnig S, Prigge M, Tolo J, Gordus A, Orger MB, Severi KE, Macklin JJ, *et al.* (2013). Genetically encoded calcium indicators for multi-color neural activity imaging and combination with optogenetics. Front Mol Neurosci 6, 2.

Cardenas C, Miller RA, Smith I, Bui T, Molgo J, Muller M, Vais H, Cheung KH, Yang J, Parker I, *et al.* (2010). Essential regulation of cell bioenergetics by constitutive InsP3 receptor Ca2+ transfer to mitochondria. Cell 142, 270–283.

Casuscelli J, Schmidt S, DeGray B, Petri ET, Celic A, Folta-Stogniew E, Ehrlich BE, Boggon TJ (2009). Analysis of the cytoplasmic interaction between polycystin-1 and polycystin-2. Am J Physiol Renal Physiol 297, F1310–F1315.

Chapin HC, Caplan MJ (2010). The cell biology of polycystic kidney disease. J Cell Biol 191, 701–710.

Chapin HC, Rajendran V, Capasso A, Caplan MJ (2009). Detecting the surface localization and cytoplasmic cleavage of membrane-bound proteins. Methods Cell Biol 94, 223–239.

Chapin HC, Rajendran V, Caplan MJ (2010). Polycystin-1 surface localization is stimulated by polycystin-2 and cleavage at the G protein-coupled receptor proteolytic site. Mol Biol Cell 21, 4338–4348.

Delmas P, Nauli SM, Li X, Coste B, Osorio N, Crest M, Brown DA, Zhou J (2004). Gating of the polycystin ion channel signaling complex in neurons and kidney cells. FASEB J 18, 740–742.

Fedeles SV, Tian X, Gallagher AR, Mitobe M, Nishio S, Lee SH, Cai Y, Geng L, Crews CM, Somlo S (2011). A genetic interaction network of five genes for human polycystic kidney and liver diseases defines polycystin-1 as the central determinant of cyst formation. Nat Genet 43, 639–647.

Gonzalez-Perrett S, Kim K, Ibarra C, Damiano AE, Zotta E, Batelli M, Harris PC, Reisin IL, Arnaout MA, Cantiello HF (2001). Polycystin-2, the protein mutated in autosomal dominant polycystic kidney disease (ADPKD), is a Ca2+-permeable nonselective cation channel. Proc Natl Acad Sci USA 98, 1182–1187.

Halvorson CR, Bremmer MS, Jacobs SC (2010). Polycystic kidney disease: inheritance, pathophysiology, prognosis, and treatment. Int J Nephrol Renovasc Dis 3, 69–83.

Hanaoka K, Qian F, Boletta A, Bhunia AK, Piontek K, Tsiokas L, Sukhatme VP, Guggino WB, Germino GG (2000). Co-assembly of polycystin-1 and -2 produces unique cation-permeable currents. Nature 408, 990–994.

Harris PC, Torres VE (2009). Polycystic kidney disease. Annu Rev Med 60, 321–337.

Harris PC, Torres VE (2014). Genetic mechanisms and signaling pathways in autosomal dominant polycystic kidney disease. J Clin Invest 124, 2315–2324.

Jaakkola P, Mole DR, Tian YM, Wilson MI, Gielbert J, Gaskell SJ, Kriegsheim A, Hebestreit HF, Mukherji M, Schofield CJ, *et al.* (2001). Targeting of HIF-α to the von Hippel-Lindau ubiquitylation complex by O_2-regulated prolyl hydroxylation. Science 292, 468–472.

Jaakkola PM, Rantanen K (2013). The regulation, localization, and functions of oxygen-sensing prolyl hydroxylase PHD3. Biol Chem 394, 449–457.

Jung IH, Park JC, Kim JC, Jeon DW, Choi SH, Cho KS, Im GI, Kim BS, Kim CS (2012). Novel application of human periodontal ligament stem cells and water-soluble chitin for collagen tissue regeneration: in vitro and in vivo investigations. Tissue Eng Part A 18, 643–653.

Kim H, Xu H, Yao Q, Li W, Huang Q, Outeda P, Cebotaru V, Chiaravalli M, Boletta A, Piontek K, *et al.* (2014). Ciliary membrane proteins traffic through the Golgi via a Rabep1/GGA1/Arl3-dependent mechanism. Nat Commun 5, 5482.

Koulen P, Cai Y, Geng L, Maeda Y, Nishimura S, Witzgall R, Ehrlich BE, Somlo S (2002). Polycystin-2 is an intracellular calcium release channel. Nat Cell Biol 4, 191–197.

Luo W, Lin B, Wang Y, Zhong J, O'Meally R, Cole RN, Pandey A, Levchenko A, Semenza GL (2014). PHD3-mediated prolyl hydroxylation of nonmuscle actin impairs polymerization and cell motility. Mol Biol Cell 25, 2788–2796.

McCormack JG, Denton RM (1979). The effects of calcium ions and adenine nucleotides on the activity of pig heart 2-oxoglutarate dehydrogenase complex. Biochem J 180, 533–544.

Menezes LF, Lin C, Zhou F, Germino GG (2016). Fatty acid oxidation is impaired in an orthologous mouse model of autosomal dominant polycystic kidney disease. EBioMedicine 5, 183–192.

Merrick D, Chapin H, Baggs JE, Yu Z, Somlo S, Sun Z, Hogenesch JB, Caplan MJ (2012). The gamma-secretase cleavage product of polycystin-1 regulates TCF and CHOP-mediated transcriptional activation through a p300-dependent mechanism. Dev Cell 22, 197–210.

Morgan AJ, Jacob R (1994). Ionomycin enhances Ca2+ influx by stimulating store-regulated cation entry and not by a direct action at the plasma membrane. Biochem J 300, 665–672.

Ong AC, Harris PC (2015). A polycystin-centric view of cyst formation and disease: the polycystin revisited. Kidney Int 88, 699–710.

Patergnani S, Suski JM, Agnoletto C, Bononi A, Bonora M, De Marchi E, Giorgi C, Marchi S, Missiroli S, Poletti F, *et al.* (2011). Calcium signaling around mitochondria associated membranes (MAMs). Cell Commun Signal 9, 19.

Pazour GJ, Rosenbaum JL (2002). Intraflagellar transport and cilia-dependent diseases. Trends Cell Biol 12, 551–555.

Qian F, Boletta A, Bhunia AK, Xu H, Liu L, Ahrabi AK, Watnick TJ, Zhou F, Germino GG (2002). Cleavage of polycystin-1 requires the receptor for egg jelly domain and is disrupted by human autosomal-dominant polycystic kidney disease 1-associated mutations. Proc Natl Acad Sci USA 99, 16981–16986.

Rizzuto R, De Stefani D, Raffaello A, Mammucari C (2012). Mitochondria as sensors and regulators of calcium signalling. Nat Rev Mol Cell Biol 13, 566–578.

Rowe I, Chiaravalli M, Mannella V, Ulisse V, Quilici G, Pema M, Song XW, Xu H, Mari S, Qian F, *et al*. (2013). Defective glucose metabolism in polycystic kidney disease identifies a new therapeutic strategy. Nat Med 19, 488–493.

Takahashi N, Kuwaki T, Kiyonaka S, Numata T, Kozai D, Mizuno Y, Yamamoto S, Naito S, Knevels E, Carmeliet P, *et al*. (2011). TRPA1 underlies a sensing mechanism for O2. Nat Chem Biol 7, 701–711.

Vander Heiden MG, Cantley LC, Thompson CB (2009). Understanding the Warburg effect: the metabolic requirements of cell proliferation. Science 324, 1029–1033.

Wodarczyk C, Rowe I, Chiaravalli M, Pema M, Qian F, Boletta A (2009). A novel mouse model reveals that polycystin-1 deficiency in ependyma and choroid plexus results in dysfunctional cilia and hydrocephalus. PLoS One 4, e7137.

Xie L, Xiao K, Whalen EJ, Forrester MT, Freeman RS, Fong G, Gygi SP, Lefkowitz RJ, Stamler JS (2009). Oxygen-regulated beta(2)-adrenergic receptor hydroxylation by EGLN3 and ubiquitylation by pVHL. Sci Signal 2, ra33.